J|A|C|S
ARTICLES
Published on Web 03/01/2006

Biosynthesis of Pipecolic Acid by RapL, a Lysine Cyclodeaminase Encoded in the Rapamycin Gene Cluster

Gregory J. Gatto, Jr.,[†] Michael T. Boyne, II,[‡] Neil L. Kelleher,[‡] and Christopher T. Walsh*,[†]

Contribution from the Department of Biological Chemistry and Molecular Pharmacology, Harvard Medical School, Boston, Massachusetts 02115, and Department of Chemistry, University of Illinois at Urbana-Champaign, Urbana, Illinois 61801

Received December 26, 2005; E-mail: christopher_walsh@hms.harvard.edu

Abstract: Rapamycin, FK506, and FK520 are immunosuppressant macrolactone natural products comprised of predominantly polyketide-based core structures. A single nonproteinogenic pipecolic acid residue is installed into the scaffold by a nonribosomal peptide synthetase that also performs the subsequent macrocyclization step at the carbonyl group of this amino acid. It has been assumed that pipecolic acid is generated from lysine by the cyclodeaminases RapL/FkbL. Herein we report the heterologous overexpression and purification of RapL and validate its ability to convert L-lysine to L-pipecolic acid by a cyclodeamination reaction that involves redox catalysis. RapL also accepts L-ornithine as a substrate, albeit with a significantly reduced catalytic efficiency. Turnover is presumed to encompass a reversible oxidation at the α-amine, internal cyclization, and subsequent re-reduction of the cyclic Δ^1-piperideine-2-carboxylate intermediate. As isolated, RapL has about 0.17 equiv of tightly bound NAD^+, suggesting that the enzyme is incompletely loaded when overproduced in *E. coli*. In the presence of exogenous NAD^+, the initial rate is elevated 8-fold with a K_m of 2.3 μM for the cofactor, consistent with some release and rebinding of NAD^+ during catalytic cycles. Through the use of isotopically labeled substrates, we have confirmed mechanistic details of the cyclodeaminase reaction, including loss of the α-amine and retention of the hydrogen atom at the α-carbon. In addition to the characterization of a critical enzyme in the biosynthesis of a medically important class of natural products, this work represents the first in vitro characterization of a lysine cyclodeaminase, a member of a unique group of enzymes which utilize the nicotinamide cofactor in a catalytic manner.

Introduction

Rapamycin, FK506, and FK520 are macrolactone natural products isolated from streptomycetes (Figure 1).[1−3] Originally identified as antifungal agents, they have since gained recognition as potent immunosuppressants and are currently in use or under investigation for use in a number of therapeutic areas, including transplant medicine, dermatology, and cardiology.[4−7] While these compounds influence different signaling cascades within the cell,[8] they share a common initial step: interaction with a class of proteins known as the FK506-binding proteins (FKBPs). FKBPs are members of the peptidyl−prolyl *cis*−*trans*-isomerase (PPIase) family;[9] the pipecolyl moieties of rapamycin and FK506/FK520 serve as substrate mimics within the active sites of these enzymes.[10−12]

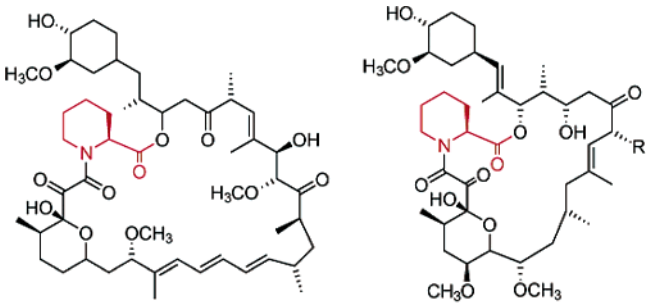

Figure 1. Structures of rapamycin, FK506, and FK520. The pipecolyl moiety is highlighted in red.

[†] Harvard Medical School.
[‡] University of Illinois at Urbana-Champaign.

(1) Vezina, C.; Kudelski, A.; Sehgal, S. N. *J. Antibiot.* **1975**, *28*, 721−726.
(2) Kino, T.; Hatanaka, H.; Miyata, S.; Inamura, N.; Nishiyama, M.; Yajima, T.; Goto, T.; Okuhara, M.; Kohsaka, M.; Aoki, H. *J. Antibiot.* **1987**, *40*, 1256−1265.
(3) Hatanaka, H.; Kino, T.; Miyata, S.; Inamura, N.; Kuroda, A.; Goto, T.; Tanaka, H.; Okuhara, M. *J. Antibiot.* **1988**, *41*, 1592−1601.
(4) Kahan, B. D. *Lancet* **2000**, *356*, 194−202.
(5) Reynolds, N. J.; Al-Daraji, W. I. *Clin. Exp. Dermatol.* **2002**, *27*, 555−561.
(6) Antin, J. H.; Kim, H. T.; Cutler, C.; Ho, V. T.; Lee, S. J.; Miklos, D. B.; Hochberg, E. P.; Wu, C. J.; Alyea, E. P.; Soiffer, R. J. *Blood* **2003**, *102*, 1601−1605.
(7) Moses, J. W.; Leon, M. B.; Popma, J. J.; Fitzgerald, P. J.; Holmes, D. R.; O'Shaughnessy, C.; Caputo, R. P.; Kereiakes, D. J.; Williams, D. O.; Teirstein, P. S.; Jaeger, J. L.; Kuntz, R. E. *N. Engl. J. Med.* **2003**, *349*, 1315−1323.
(8) Schreiber, S. L.; Crabtree, G. R. *Harvey Lect.* **1995**, *91*, 99−114.
(9) Schiene-Fischer, C.; Yu, C. *FEBS Lett.* **2001**, *495*, 1−6.
(10) Albers, M. W.; Walsh, C. T.; Schreiber, S. L. *J. Org. Chem.* **1990**, *55*, 4984−4986.

10.1021/ja0587603 CCC: $33.50

The biosynthesis of most of the core macrocycle of rapamycin by its producer strain, *Streptomyces hygroscopicus*, proceeds via a multimodular array of polyketide synthases (PKSs) encoded by the *rapA*, *rapB*, and *rapC* genes.[13] The nonproteinogenic pipecolic acid residue is added to the completed polyketide chain by the action of a single nonribosomal peptide synthetase module, RapP, which is also presumed to be responsible for the macrolactonization of the chain (Figure 2A).[14−16] Incubation of the rapamycin producer strain with labeled metabolites had implicated lysine as the source of the pipecolate moiety,[17] a proposal supported by the identification of the *rapL* gene within the rapamycin gene cluster. On the basis of its homology to the ornithine cyclodeaminases (OCDs) (Figure 2B), RapL was predicted to act as a lysine cyclodeaminase, catalyzing the direct formation of L-pipecolic acid from L-lysine (Figure 2C).[18] Additional evidence for this role of RapL came from the observation that chromosomal disruption of the *rapL* gene yields a *S. hygroscopicus* strain which requires the exogenous addition of L-pipecolate for rapamycin production.[19]

In addition to RapL and its ortholog in the FK506- and FK520-producer strains, FkbL, only two other lysine cyclodeaminases have been identified: VisC and TubZ, from the biosynthetic pathways of virginiamycin S[20] and tubulysin,[21] respectively. While little is known about the in vitro activity of lysine cyclodeaminases, there have been a number of published reports on the identification and characterization of OCDs. Costilow and co-workers first described such activity on enzyme purified from *Clostridium sporogenes*.[22−24] They identified NAD^+ as a key cofactor in the transformation of ornithine to proline and noted that the α-amino group, as opposed to that at the δ-position, is lost during the reaction.[24] Further enzymatic characterization was reported on OCDs identified in the Ti plasmids of the tumor-inducing bacterium *Agrobacterium tumefaciens*.[25−27] In addition, the cocrystal structure of *Pseudomonas putida* OCD with NADH and ornithine was recently published.[28] On the basis of these studies, a reaction mechanism for OCD had been proposed[29] and later revised (Figure 2B).[28] According to this mechanism, the α-amino group of L-ornithine is first oxidized to an imine in an NAD^+-dependent manner. Attack of the δ-amine at the imino carbon yields a tetrahedral intermediate which subsequently undergoes loss of ammonia to form the cyclic imino acid, Δ^1-pyrroline-2-carboxylic acid. Reduction of the imino group by the previously formed NADH yields the product, L-proline, and recycles the cofactor back to oxidized NAD^+.

In most enzyme-catalyzed reactions that require $NAD(P)^+$ or NAD(P)H, the pyridine nucleotide acts as a cosubstrate. The mechanisms shown in Figure 2B and 2C are unusual in that the nicotinamide cofactor is recycled to its original oxidation state. Catalytic usage of NAD^+, previously referred to as a "complex NAD^+-dependent transformation",[30] has been proposed in several other enzymes, including UDP-galactose 4-epimerase,[31] *S*-adenosylhomocysteine hydrolase,[32] and *myo*-inositol-1-phosphate synthase.[33] Characteristic of the mechanisms of these enzymes is the oxidation of substrate by NAD^+ to transiently activate a bond that is otherwise not reactive. Typically, these enzymes are multimeric and bind cofactor very tightly so as to prevent the dissociation of NADH during the reaction cycle.

Because of its unusual mechanism and its importance in the biosynthesis of a key functional component of the macrolide immunosuppressant rapamycin, we sought to characterize the in vitro enzymatic activity of RapL. We report here the heterologous expression and purification of RapL from *E. coli* and demonstration of its lysine cyclodeaminase activity. RapL discriminates L-lysine from L-ornithine by approximately 100-fold and requires exogenous NAD^+ for full activity. Using spectroscopic and chromatographic methods, we have determined that the purified enzyme is present in three forms: NAD^+-bound, NADH-bound, and cofactor-free. In addition, the similarity between the mechanisms of RapL and the OCDs has been confirmed through the use of isotopically labeled substrates and mass spectrometry. Finally, we have characterized the inhibitory properties of several compounds previously proposed to interrupt RapL function in precursor-directed biosynthetic experiments.[34−36]

Materials and Methods

Materials. Chemically competent TOP10 and BL21(DE3) *E. coli* were obtained from Invitrogen; pET28a was purchased from Novagen. All restriction endonucleases and T4 DNA ligase were obtained from New England Biolabs. Synthetic DNA oligonucleotides were purchased from Integrated DNA Technologies and used without further purification. PCRs were run with Pfu Turbo DNA polymerase from Stratagene, on a Stratagene RoboCycler Gradient 96. Pre-cast SDS−PAGE gels and protein molecular weight markers were obtained from BioRad. Ni−NTA chromatography resin was purchased from Qiagen. L-[U-^{14}C]-

(11) Fischer, S.; Michnick, S.; Karplus, M. *Biochemistry* **1993**, *32*, 13830−13837.
(12) Van Duyne, G. D.; Standaert, R. F.; Karplus, P. A.; Schreiber, S. L.; Clardy, J. *J. Mol. Biol.* **1993**, *229*, 105−124.
(13) Schwecke, T.; Aparicio, J. F.; Molnár, I.; König, A.; Khaw, L. E.; Haydock, S. F.; Oliynyk, M.; Caffrey, P.; Cortés, J.; Lester, J. B.; Böhm, G. A.; Staunton, J.; Leadlay, P. F. *Proc. Natl. Acad. Sci. U.S.A.* **1995**, *92*, 7839−7843.
(14) Nielsen, J. B.; Hsu, M.-J.; Byrne, K. M.; Kaplan, L. *Biochemistry* **1991**, *30*, 5789−5796.
(15) König, A.; Schwecke, T.; Molnár, I.; Böhm, G. A.; Lowden, P. A. S.; Staunton, J.; Leadlay, P. F. *Eur. J. Biochem.* **1997**, *247*, 526−534.
(16) Gatto, G. J., Jr.; McLoughlin, S. M.; Kelleher, N. L.; Walsh, C. T. *Biochemistry* **2005**, *44*, 5993−6002.
(17) Paiva, N. L.; Demain, A. L.; Roberts, M. F. *Enzyme Microb. Technol.* **1993**, *15*, 581−585.
(18) Molnár, I.; Aparicio, J. F.; Haydock, S. F.; Khaw, L. E.; Schwecke, T.; König, A.; Staunton, J.; Leadlay, P. F. *Gene* **1996**, *169*, 1−7.
(19) Khaw, L. E.; Bohm, G. A.; Metcalfe, S.; Staunton, J.; Leadlay, P. F. *J. Bacteriol.* **1998**, *180*, 809−814.
(20) Namwat, W.; Kamioka, Y.; Kinoshita, H.; Yamada, Y.; Nihira, T. *Gene* **2002**, *286*, 283−290.
(21) Sandmann, A.; Sasse, F.; Müller, R. *Chem. Biol.* **2004**, *11*, 1071−1079.
(22) Costilow, R. N.; Laycock, L. *J. Biol. Chem.* **1971**, *246*, 6655−6660.
(23) Muth, W. L.; Costilow, R. N. *J. Biol. Chem.* **1974**, *249*, 7457−7462.
(24) Muth, W. L.; Costilow, R. N. *J. Biol. Chem.* **1974**, *249*, 7463−7467.
(25) Sans, N.; Schröder, G.; Schröder, J. *Eur. J. Biochem.* **1987**, *167*, 81−87.
(26) Sans, N.; Schindler, U.; Schröder, J. *Eur. J. Biochem.* **1988**, *173*, 123−130.
(27) Schindler, U.; Sans, N.; Schröder, J. *J. Bacteriol.* **1989**, *171*, 847−854.
(28) Goodman, J. L.; Wang, S.; Alam, S.; Ruzicka, F. J.; Frey, P. A.; Wedekind, J. E. *Biochemistry* **2004**, *43*, 13883−13891.
(29) Walsh, C. *Enzymatic Reaction Mechanisms*; W. H. Freeman & Co.: New York, 1979.
(30) Frey, P. A. Complex pyridine nucleotide-dependent transformations. In *Pyridine Nucleotide Coenzymes, Part* B; Dolphin, D., Poulson, R., Avramovic, O., Eds.; Wiley-Interscience: New York, 1987; pp 461−511.
(31) Frey, P. A. *FASEB J.* **1996**, *10*, 461−470.
(32) Turner, M. A.; Yang, X.; Yin, D.; Kuczera, K.; Borchardt, R. T.; Howell, P. L. *Cell Biochem. Biophys.* **2000**, *33*, 101−125.
(33) Jin, X.; Geiger, J. H. *Acta Crystallogr.* **2003**, *D59*, 1154−1164.
(34) Kojima, I.; Demain, A. L. *J. Ind. Microbiol. Biotechnol.* **1998**, *20*, 309−316.
(35) Graziani, E. I.; Ritacco, F. V.; Summers, M. Y.; Zabriskie, T. M.; Yu, K.; Bernan, V. S.; Greenstein, M.; Carter, G. T. *Org. Lett.* **2003**, *5*, 2385−2388.
(36) Ritacco, F. V.; Graziani, E. I.; Summers, M. Y.; Zabriskie, T. M.; Yu, K.; Bernan, V. S.; Carter, G. T.; Greenstein, M. *Appl. Environ. Microbiol.* **2005**, *71*, 1971−1976.

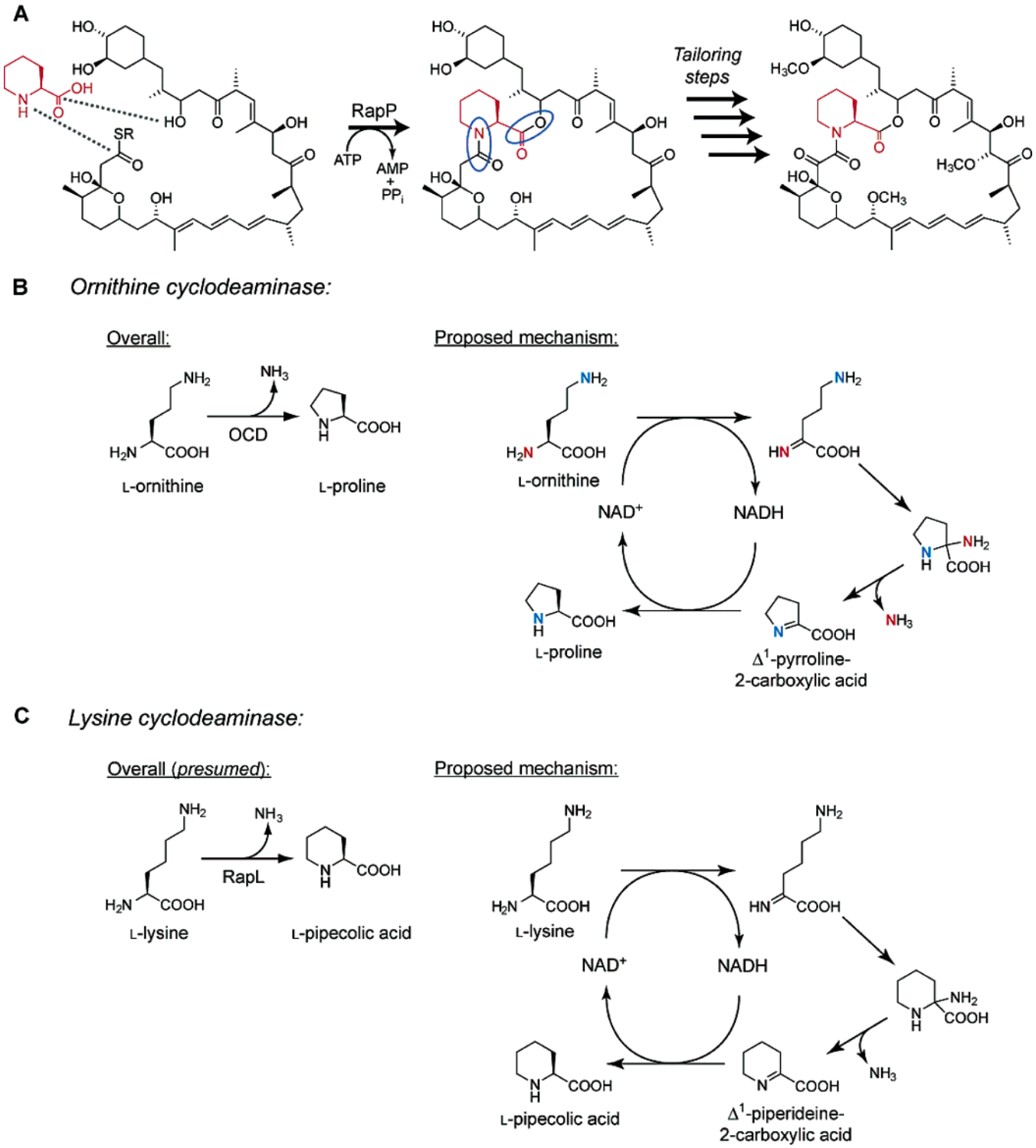

Figure 2. (A) Schematic of pipecolate (red) incorporation into the rapamycin polyketide chain. Through the formation of pipecolyl-AMP and pipecolyl-*S*-enzyme intermediates (not shown), RapP catalyzes the formation of two bonds in the final product (circled in blue) that are critical for immunosuppressant activity. Post-PKS/NRPS tailoring steps complete the biosynthesis. (B) The overall reaction (left) and proposed mechanism (right) of OCD.[22,24,28] In the mechanism, the α-NH_2 (red) and δ-NH_2 (blue) are highlighted. (C) The presumed overall reaction and mechanism for RapL, a lysine cyclodeaminase.

Lysine and L-[U-^{14}C]ornithine were obtained from Amersham Biosciences. D-[1-^{14}C]Lysine was obtained from American Radiolabeled Chemicals. BAS−IIIs phosphorimager plates were obtained from Fuji. DNA sequencing and quantitative amino acid analysis were performed at the Molecular Biology Core Facilities at the Dana-Farber Cancer Institute. UV/vis spectra were measured on an Hewlett-Packard 8453 spectrophotometer. (*R*)-(−)-Nipecotic acid and (*S*)-(+)-nipecotic acid were obtained from TCI America. L-[α-^{15}N]Lysine and L-[ε-^{15}N]lysine were purchased from Cambridge Isotope Laboratories. DL-[2,3,3,4,4,5,5,6,6-d_9]Lysine and DL-[2,3,3,4,4,5,5,6,6-d_9]pipecolic acid were obtained from C/D/N Isotopes. All other materials were purchased from Sigma-Aldrich.

Overexpression and Purification of RapL. The open reading frame of the *rapL* gene was amplified from a cosmid containing the rapamycin biosynthetic cluster (kindly provided by Dr. Christopher Reeves, Kosan Biosciences) using the following primers: 5′-GGG TTT CCA TAT

GCA GAC CAA GGT TCT GTG CCA GCG-3′ (forward) and 5′-GGT ATA CGA ATT CCT ACA GCG AGT ACG GAT CGA GGA CG-3′ (reverse). *Nde*I and *Eco*RI sites are underlined. The resulting PCR product was digested with *Nde*I and *Eco*RI, purified by agarose gel electrophoresis, and ligated into similarly digested pET28a to generate the expression construct, pET28a-RapL(N-His), encoding RapL fused to an N-terminal hexahistidine tag of the following sequence: $^{+}H_3N$-MGSSHHHHHHSSGLVPRGSH. The identity of pET28a-RapL(N-His) was confirmed by DNA sequencing.

The *rapL* expression plasmid was transformed into the *E. coli* strain BL21(DE3) and grown in LB media supplemented with 30 μg/mL kanamycin. Each liter of culture was inoculated with 10 mL of overnight starter culture. Cultures were grown at 25 °C to an OD_{600} of 0.4−0.6, induced with 60 μM IPTG, then incubated at 25 °C for an additional 16 h. Cells were harvested by centrifugation (20 min at 6000*g*), resuspended in lysis buffer (400 mM NaCl, 25 mM Tris pH 8.0, 10% glycerol), and lysed by two passages through a French press at 16 000 psi. Ni−NTA resin (1 mL per liter of culture) and 2 mM imidazole were added to the clarified lysate and allowed to batch bind for 2 h at 4 °C. The resin was washed with 5 column volumes of 2 mM imidazole in lysis buffer. Protein was eluted with a step gradient of increasing imidazole concentrations in lysis buffer (5, 20, 40, 60, 200, 500 mM). The RapL protein product typically eluted in the 40 and 60 mM fractions, which were pooled and dialyzed at 4 °C in two steps: 4 h in 100 mM NaCl, 50 mM Tris pH 8.0, 1 mM EDTA, 10% glycerol; followed by 4 h in 100 mM NaCl, 50 mM Tris pH 8.0, 1 mM TCEP, 10% glycerol. Concentrated protein solutions were stored at −80 °C. Protein concentrations were determined by quantitative amino acid analysis.

Characterization of RapL Cyclodeaminase activity. To determine kinetic parameters with respect to lysine, L-[U-^{14}C]lysine (10−500 μM; 4 nCi/μL) was incubated in a final volume of 25 μL with 1.7 μM RapL, 100 μM NAD^+, 100 mM HEPES (pH 8.0), and 1 mg/mL BSA at 30 °C. Reactions were run in triplicate and initiated by the addition of enzyme. At time points of 5, 15, and 30 min, 5 μL was withdrawn from the reaction mixture, quenched in 10 μL of methanol, and stored at −20 °C for at least 10 min. The quenched reactions were spun at 16 000*g* for 10 min, and 1 μL of the supernatant was spotted on a cellulose thin layer chromatography (TLC) plate (Merck KGaA; Darmstadt, Germany). The TLC plate was developed in 3:1 *n*-propanol: 30% NH_4OH and exposed to a BAS−IIIs phosphorimager plate for 16 h at room temperature. Plates were read using a Typhoon 9400 phosphorimager (GE Healthcare), and the resulting image was analyzed by ImageQuant v5.2 (Molecular Dynamics). When it was necessary to run authentic L-pipecolic acid standard, unlabeled sample was used, and that portion of the plate was stained with ninhydrin. A known amount of radioactivity was overlaid onto the ninhydrin-stained compound prior to autoradiography. The ratio of pipecolic acid (R_f = 0.44) to lysine (R_f = 0.10) signals was used to calculate the amount of product formed in each reaction. Initial velocity data were fitted to the Michaelis−Menten equation in Mathematica (Wolfram Research) to obtain estimates for k_{cat} and K_m.

For determination of kinetic parameters with respect to ornithine, the same assay conditions were used as above, with the exception that L-[U-^{14}C]lysine was replaced with L-[U-^{14}C]ornithine (0.2−1.3 mM; 25 nCi/μL). For determination of kinetic parameters with respect to NAD^+, the concentration of L-[U-^{14}C]lysine was kept constant at 150 μM (10 nCi/μL), and the concentration of NAD^+ was varied from 0.1 to 50 μM.

To determine the chirality of the pipecolic acid product, the RapL reaction was run as above in the presence of 200 μM L-[U-^{14}C]lysine (20 nCi/μL). After 100 min, the reaction was quenched with 2 reaction volumes of methanol. Ten microliters of this mixture was analyzed by radio-HPLC on a Beckman-Coulter System Gold fitted with a Phenomenex Chirex D-penicillamine column (5 μm, 250 × 4.6 mm) and equipped with an inline IN/US β-RAM Model 3 radio flow detector. The L and D isomers of pipecolic acid were separated in isocratic conditions of 1 mM copper(II) sulfate in water.

Determination of NAD^+ versus NADH Content of RapL. The content of NAD^+ and NADH bound to purified RapL was estimated using an HPLC method based on that described by Yuan and Borchardt.[37] A quantity of 220 μL of an 85 μM solution of purified RapL (19 nmol) was precipitated with 3 volumes of 95% ethanol. The supernatant was flash frozen in liquid N_2 and lyophilized for 16 h. The residue was dissolved in 100 μL of water and analyzed by HPLC on a Beckman-Coulter System Gold fitted with an Alltech Econosphere C18 column (5 μm, 250 × 4.6 mm) with monitoring at 260 and 340 nm. NAD^+ and NADH separated in isocratic conditions at 2.5% methanol in 0.1 M sodium phosphate buffer (pH 7.0). Standard curves were generated with authentic NAD^+ and NADH so as to correlate peak area with cofactor amount.

Characterization of RapL Inhibitors. The cyclodeaminase assay was run as described above, with the concentration of L-[U-^{14}C]lysine fixed at 100 μM (10 nCi/μL) and the addition of either (*R*)-(−)-nipecotic acid, (*S*)-(+)-nipecotic acid, or thiazolidine-2-carboxylic acid in concentrations ranging from 10 nM to 10 mM in 10-fold increments. Reactions were run in triplicate. Using Mathematica, reaction velocities as a function of inhibitor concentration were fit to the following expression:

$$\frac{V_i}{V_o} = \frac{1}{1 + \frac{[I]}{IC_{50}}}$$

where V_i and V_o are the initial velocities in the presence and absence of inhibitor, respectively, [I] is the inhibitor concentration, and IC_{50} is the concentration of inhibitor required to yield a half-maximal response.[38]

Fmoc Derivatization of RapL Reaction Mixtures. One millmole L-lysine was incubated at 30 °C with 10 μM RapL, 5 mM Tris (pH 8.0), 1 mg/mL BSA, and 100 μM NAD^+ (total volume = 75 μL) for 16 h. The reaction was quenched with two reaction volumes of acetonitrile, stored at −20 °C for at least 10 min, and spun at 16 000*g* for 10 min. Derivatization of the quenched reaction was carried out using a procedure based on that described by Fabiani et al.[39] One hundred fifty microliters of the supernatant was withdrawn and added to 50 μL of 200 mM borate (pH 8). Twenty microliters of 10 mM 9-fluorenylmethyl chloroformate was added, and the reaction was allowed to proceed at room temperature for 30 min. To remove any remaining derivatizing reagent, 40 μL of 100 mM 1-aminoadamantane was added, and the mixture was kept at room temperature for an additional 5 min. The reaction was centrifuged at 16 000*g* for 1 min, then 150 μL of the supernatant was injected onto a Beckman-Coulter System Gold HPLC system fitted with an Alltech Alltima C18 column (5 μm; 250 × 4.6 mm) and equipped with an inline Jasco FP-2020 Plus fluorescence detector. Fmoc-derivatized compounds were separated with a gradient of 30−100% acetonitrile in aqueous 0.1% trifluoroacetic acid over 70 min and detected using both absorbance at 263 nm and fluorescence emission at 630 nm (λ_{ex} = 263 nm).[40] The peak corresponding to Fmoc-pipecolic acid was collected, flash frozen in liquid N_2, lyophilized overnight, resuspended in 30% acetonitrile, and analyzed by mass spectrometry.

Mass Spectrometric Analysis. Data were collected on a 7 T LTQ-FTMS (Thermo-Finnigan) with direct infusion through an electrospray source. Samples were diluted in 50 μL of water:methanol:acetic acid

(37) Yuan, C. S.; Borchardt, R. T. *J. Biol. Chem.* **1995**, *270*, 16140−16146.
(38) Copeland, R. A. *Enzymes: A Practical Introduction to Structure, Mechanism, and Data Analysis*, 2nd ed.; Wiley-VCH: New York, 2000.
(39) Fabiani, A.; Versari, A.; Parpinello, G. P.; Castellari, M.; Galassi, S. *J. Chromatogr. Sci.* **2002**, *40*, 14−18.
(40) Bank, R. A.; Jansen, E. J.; Beekman, B.; te Koppele, J. M. *Anal. Biochem.* **1996**, *240*, 167−176.

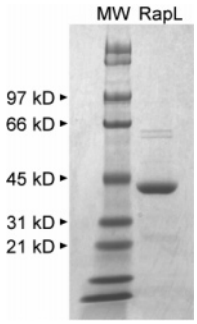

Figure 3. SDS−PAGE analysis (4−15% Tris-HCl) of RapL fused to an N-terminal hexahistidine tag (expected molecular weight: 38.4 kDa).

(49:49:2, v:v:v), and FTMS scans were summed for 3 min at a flow rate of 3 μL/min (~180 scans). The data were analyzed using Qual Browser (version 1.4 SR1) in Xcalibur to acquire accurate intact masses (within 5 ppm).

Results

Cloning, Overexpression, and Purification of RapL. The open reading frame of *rapL* was amplified from a cosmid containing the entire rapamycin biosynthetic gene cluster (kindly provided by Kosan Biosciences) and cloned into pET28a to yield a construct designed to express RapL fused to an N-terminal hexahistidine tag. Upon sequencing of this construct, seven discrepancies with the published *rapL* nucleotide sequence[13] were identified. Of these, two were silent (G285 → C and G357 → C), while the remaining five resulted in changes in the predicted amino acid sequence: C148 → A (Pro50Thr), G250 → C (Glu84Gln), G305 → A (Gly102Asp), T379 → G (Ser127Ala), and A385 → G (Thr129Ala). We confirmed that these nucleotide substitutions were present in the original cosmid and not introduced during the amplification reaction. Given the solubility and catalytic activity exhibited by the expressed protein product (vide infra), we presume these changes to reflect either errors in the published sequence or genotypic variations in the producer strains. Overexpression of His_6-tagged RapL from an *E. coli* BL21(DE3) strain bearing pET28a-RapL(NHis) was achieved by induction with 60 μM IPTG and overnight growth at 25 °C. The crude cell lysate was purified by Ni−NTA chromatography, from which we obtained approximately 8 mg of >95% pure RapL per liter of culture (Figure 3).

Steady-State Kinetics and Substrate Specificity of the RapL Cyclodeaminase Reaction. The activity of RapL was measured by cellulose thin layer chromatography (TLC) with ^{14}C-labeled L-lysine substrate using conditions similar to those reported for *A. tumefaciens* OCD.[25] When 200 μM L-lysine was incubated with 1.7 μM RapL and 100 μM NAD^+ at 30 °C, we observed a new spot with a retention factor (R_f) consistent with authentic pipecolic acid. The intensity of this spot increased in a time-dependent manner (Figure 4A). By comparing the chiral radio-HPLC elution profile of the RapL reaction with that of cold L- and D-pipecolic acid standards, we are able to assign the stereochemistry of the radiolabeled pipecolic acid product as L (Figure 4B). Steady-state kinetic analysis of this reaction yielded a K_m for L-lysine of 46 ± 4 μM and a k_{cat} of 0.61 ± 0.02 min^{-1}, resulting in a k_{cat}/K_m of 13 ± 1 mM^{-1} min^{-1} (Figure 4C). We further explored the substrate specificity of RapL by replacing L-lysine with either L-ornithine or D-lysine. A linear dependence of the initial velocity of proline formation upon L-ornithine concentration was observed at substrate concentrations up to 1.3 mM (Figure 4D), yielding a k_{cat}/K_m of 0.14 ± 0.02 mM^{-1} min^{-1}. No pipecolic acid formation was detected when D-lysine was used in place of its enantiomer.

Cofactor Requirements for Cyclodeaminase Activity. To determine the cofactor specificity of RapL, initial velocities of pipecolic acid formation were determined in the presence of 150 μM L-lysine, 1.7 μM RapL, and either 100 μM NAD^+, 100 μM $NADP^+$, 100 μM NADH, or no additional cofactor (Figure 5A). The dependence of full cyclodeaminase activity

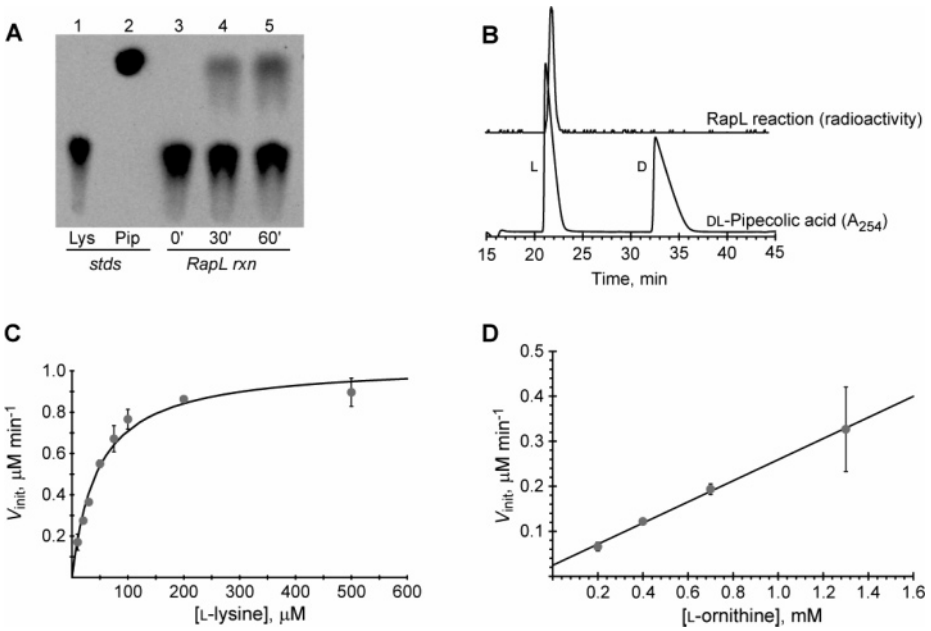

Figure 4. (A) Thin layer chromatography of L-lysine (lane 1) and L-pipecolic acid (lane 2) standards, and a time course of the RapL reaction at 0, 30, and 60 min (lanes 3, 4, and 5). (B) Chiral radio-HPLC of the RapL reaction run in the presence of 200 μM L-[U-^{14}C]lysine, measured by ^{14}C radioactivity (top trace) and elution profile of cold DL-pipecolic acid standard using the same solvent conditions as the top trace, measured by UV absorbance at 254 nm (bottom trace). (C) Plot of initial velocity versus L-lysine concentration, with the best-fit curve to the Michaelis−Menten equation. (D) Plot of initial velocity versus L-ornithine concentration, with the best fit to a linear equation. For parts (C) and (D), error bars are drawn at one standard deviation.

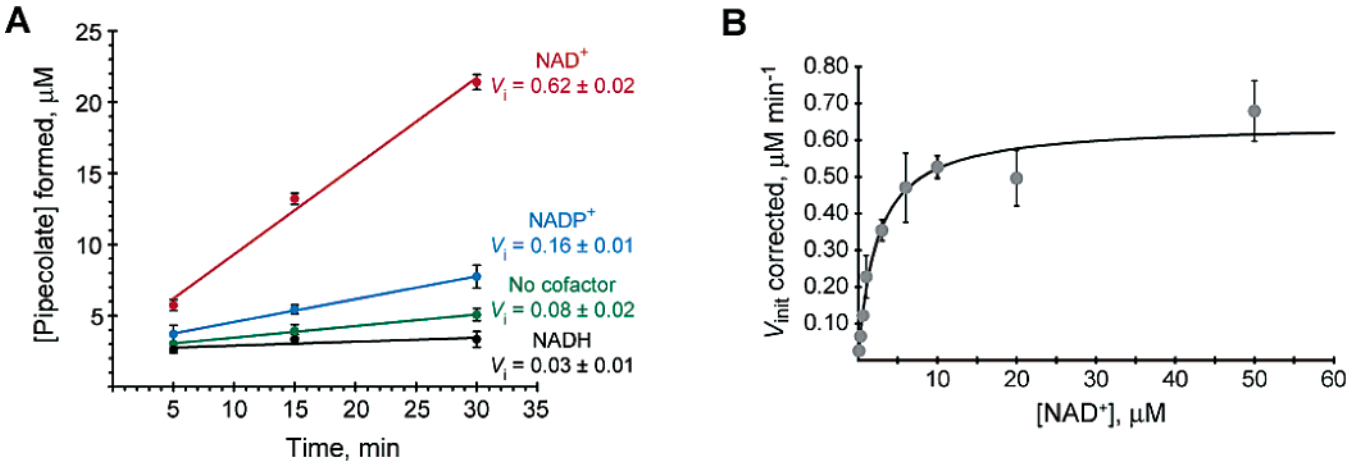

Figure 5. (A) Plot of time-dependent product formation, measured at 150 μM L-lysine in the presence of either 100 μM NAD^+ (red), 100 μM $NADP^+$ (blue), 100 μM NADH (black), or no added cofactor (green). Fitted initial velocities are reported in units of μM min^{-1}. (B) Plot of initial velocity, corrected for the rate of product formation in the absence of cofactor, versus NAD^+ concentration, with the best-fit curve to the Michaelis−Menten equation. Error bars for both (A) and (B) are drawn at one standard deviation.

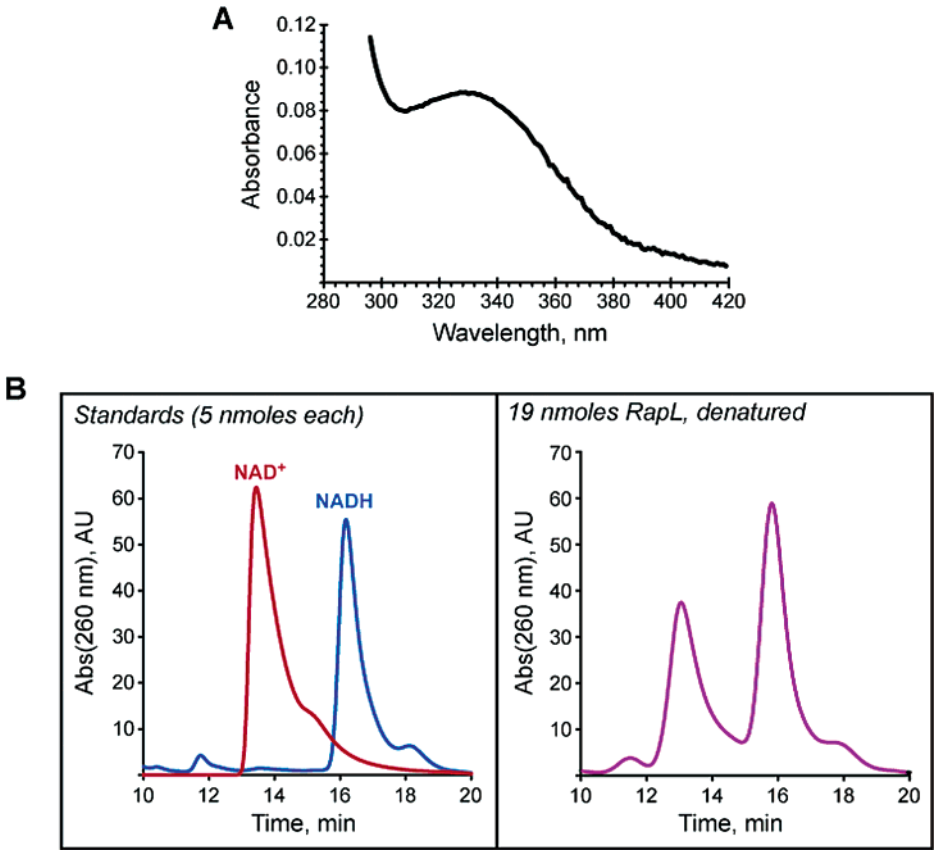

Figure 6. (A) UV/vis absorption spectrum of RapL. (B) HPLC separation of NAD^+ and NADH standards (left panel: red and blue traces, respectively), and elution profile of supernatant from denatured RapL (right panel).

upon the addition of NAD^+ enabled the determination of steady-state kinetics with respect to this component. After correction for the low level of pipecolate formation in the absence of added cofactor, Michaelis−Menten behavior was observed when initial velocity was measured in the presence of varying concentrations of NAD^+ (Figure 5B). From these data, an apparent K_m of 2.3 ± 0.4 μM for NAD^+ was obtained.

Identity of Cofactors Present in Purified RapL. Given the low level of pipecolate formation by RapL in the absence of added cofactor (Figure 5A), we sought to ascertain the profile of cofactors bound to the purified recombinant enzyme. First, UV/visible spectroscopy of RapL revealed an absorption peak near 340 nm (Figure 6A). This peak is consistent with the presence of enzyme-bound NADH since oxidized nicotinamide has no absorption at this wavelength. Second, an HPLC method[37] designed to separate NAD^+ from NADH was applied to 19 nanomoles of RapL denatured with ethanol. As shown in Figure 6B, peaks with retention times consistent with authentic NAD^+ and NADH were observed. Preparation of standard curves correlating cofactor amount with peak area enabled the quantitation of cofactor present in this RapL sample: 0.17 mol NAD^+/mol RapL and 0.35 mol NADH/mol RapL.

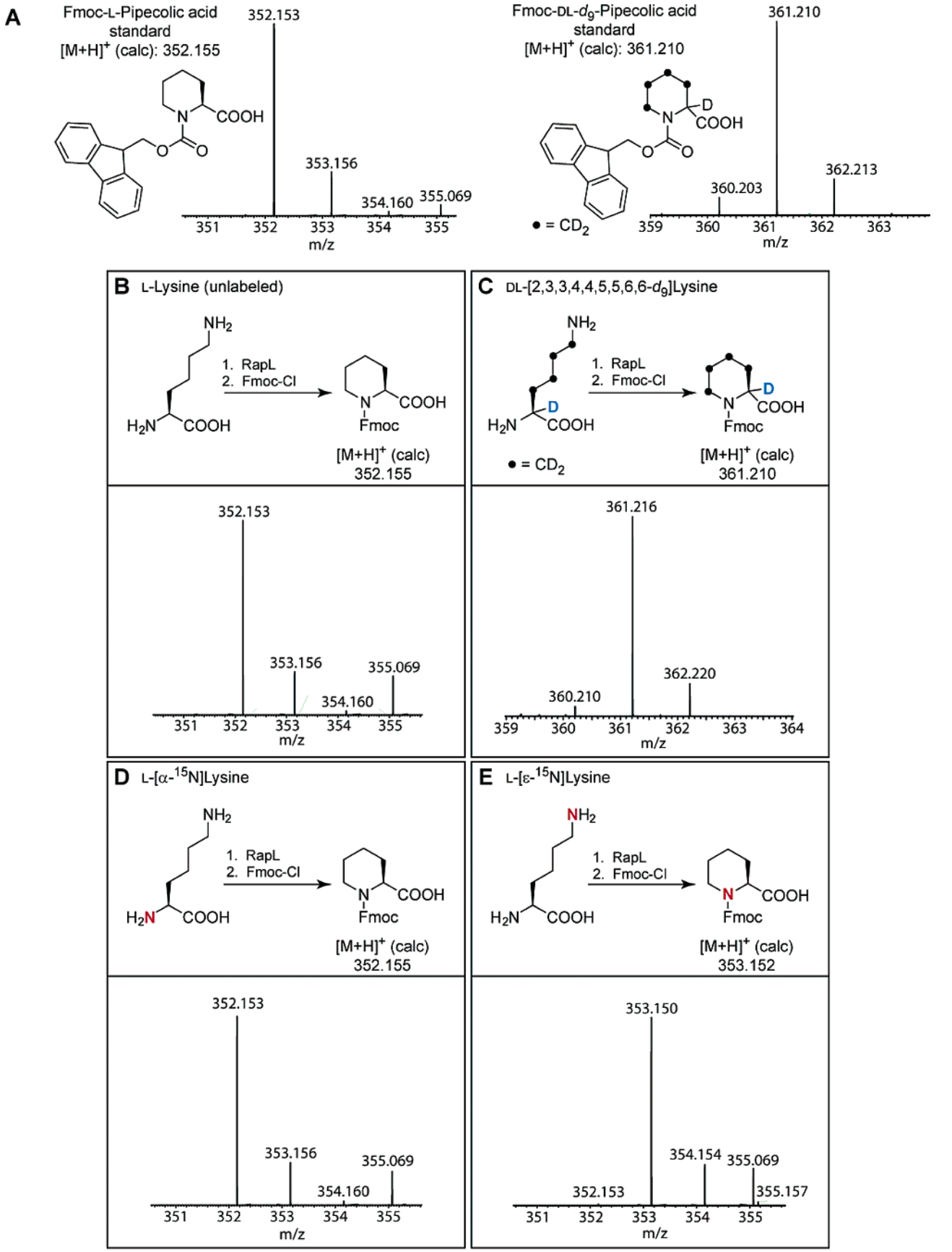

Figure 7. LTQ-FTMS analysis of the (A) Fmoc-L-pipecolic acid (left) and Fmoc-DL-d_9-pipecolic acid (right) standards, and the isolated Fmoc-pipecolic acid product from the cyclodeaminase reactions run in the presence of (B) unlabeled L-lysine, (C) DL-[2,3,3,4,4,5,5,6,6-d_9]lysine, (D) L-[α-^{15}N]lysine, and (E) L-[ϵ-^{15}N]lysine. For parts (B), (C), (D), and (E), the top panel shows the substrate and proposed structure of the derivatized product, while the bottom panel shows the mass spectrum of the isolated Fmoc-pipecolic acid product. ^{15}N atoms are colored red, and deuterium atoms are colored blue.

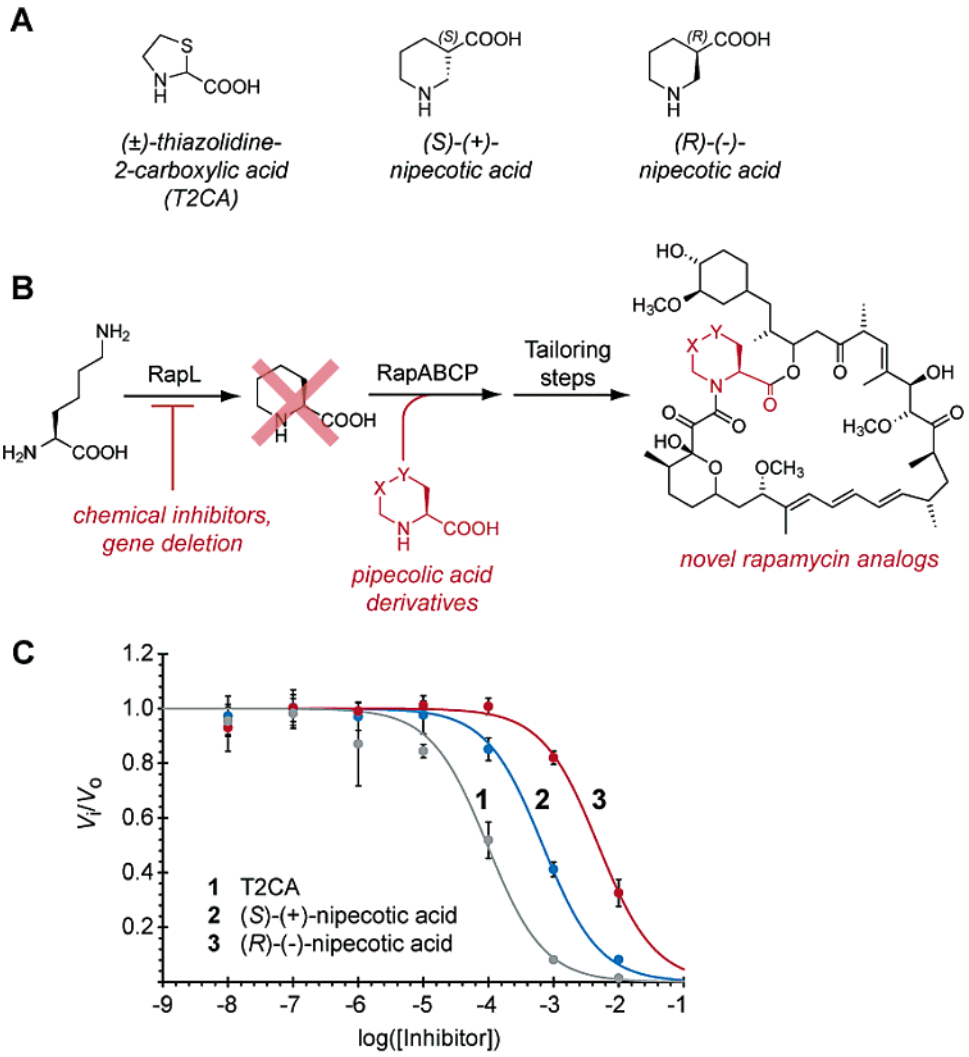

Figure 8. (A) Chemical structures of (±)-thiazolidine-2-carboxylic acid, (*S*)-(+)-nipecotic acid, and (*R*)-(−)-nipecotic acid. (B) Schematic of precursor-directed biosynthesis of rapamycin analogues after manipulation of RapL by genetic or chemical methods. (C) Dose−response curves for T2CA (gray), (*S*)-(+)-nipecotic acid (blue), and (*R*)-(−)-nipecotic acid (red). Error bars are drawn at one standard deviation.

Dissection of RapL Mechanism Using Isotopically Labeled Substrates. On the basis of its homology to the ornithine cyclodeaminases, RapL is presumed to act by a mechanism similar to that shown in Figure 2B. To test this proposed mechanism (Figure 2C), we utilized mass spectrometric analysis of the pipecolic acid formed when RapL is incubated with isotopically labeled lysine substrates. Treatment of the deproteinized assay mixture with 9-fluorenylmethyl chloroformate (Fmoc-Cl) converted any available primary and secondary amines to the corresponding Fmoc-carbamate. From this reaction mixture, the Fmoc-pipecolic acid product was easily purified by reversed-phase HPLC. Analysis of derivatized product isolated in this manner on a 7T LTQ-FT mass spectrometer yielded an $[M + H]^+$ of 352.153 (Figure 7B), identical to the value obtained for the commercially available Fmoc-L-pipecolic acid standard (Figure 7A, left).

To determine the selectivity of amine loss from the substrate, the above assay method was applied to lysine labeled with ^{15}N at either the α- or the ϵ-position. Incubation of L-[α-^{15}N]lysine with RapL, with subsequent derivatization, yielded Fmoc-pipecolic acid with an $[M + H]^+$ of 352.153 (Figure 7D), identical to that isolated from the reaction of RapL with unlabeled substrate (Figure 7B). By contrast, when L-[ϵ-^{15}N]-lysine was used in the same procedure, the observed $[M + H]^+$ of the isolated Fmoc-pipecolic acid peak was 353.150, 1 Da greater than that observed for the α-labeled and unlabeled reactions (Figure 7E).

In addition, we sought to determine if the hydrogen atom at the α-position of lysine is exchanged with solvent over the course of the cyclodeaminase reaction. Lack of observable exchange would be consistent with the participation of this hydrogen in the redox chemistry with the nicotinamide cofactor. Toward this end, we ran the RapL assay in the presence of DL-[2,3,3,4,4,5,5,6,6-d_9]lysine. Examination of the isolated Fmoc-pipecolic acid peak from this reaction yielded an $[M + H]^+$ of 361.210 (Figure 7C). This value is identical to that observed for the Fmoc-[2,3,3,4,4,5,5,6,6-d_9]pipecolic acid standard (Figure 7A, right), obtained by Fmoc derivatization of commercially available perdeutero-pipecolic acid.

Inhibition of RapL by Nipecotic Acids and Thiazolidine-2-carboxylic Acid. It has been previously reported that treatment of rapamycin producer strains of *S. hygroscopicus* with either (±)-thiazolidine-2-carboxylic acid (T2CA)[34] or (±)-nipecotic acid[35,36] (Figure 8A) enables the formation of rapamycin variants

when supplied with pipecolic acid derivatives (Figure 8B). Presumably, these compounds act on RapL to block pipecolic acid biosynthesis. To test this hypothesis directly, we determined the ability of the two stereoisomers of nipecotic acid as well as T2CA to inhibit the in vitro activity of RapL. Dose−response curves were obtained by measurement of initial reaction velocity in the presence of inhibitor concentrations spanning 7 orders of magnitude from 10 nM to 10 mM (Figure 8C). The fitted IC_{50} values for the stereoisomers of nipecotic acid were 680 ± 70 μM and 4.8 ± 0.5 mM for the (*S*) and (*R*) configurations, respectively. The fitted IC_{50} value for T2CA was 96 ± 16 μM.

Discussion

The core structure of the macrolide immunosuppressants rapamycin, FK506, and FK520 is predominantly polyketide in origin, with the exception of a single pipecolic acid residue. This amino acyl group is installed by the nonribosomal peptide synthetase RapP/FkbP and is crucial for the interaction of these molecules with their targets, the FKBPs. The positioning of the pipecolyl group as a substrate mimic within the PPIase active site serves as a critical determinant for the subnanomolar affinity of rapamycin for FKBP.[41]

Since the pipecolyl group is installed by an NRPS module, one would anticipate that L-pipecolic acid is the substrate for the activating adenylation step typically observed in this class of megasynthetases. Indeed, this has been demonstrated in vitro for both RapP and FkbP.[14−16] Lysine has been implicated as the precursor of this nonproteinogenic amino acid based on feeding studies with isotopically labeled metabolites[17] and the identification of the *rapL*/*fkbL* genes within the biosynthetic clusters for these compounds.[18,42,43] RapL bears a close resemblance to ornithine cyclodeaminases, enzymes which directly convert ornithine to proline. On the basis of this homology, it has been proposed that RapL catalyzes the analogous conversion of lysine to pipecolic acid. With an appreciation for the importance of the pipecolyl group in the activity of these compounds, the unique nature of the cyclodeaminase reaction, and recent interest in the disruption of RapL for the engineered biosynthesis of derivatized macrolides, we report here the heterologous overexpression and purification of RapL and the first in vitro characterization of its lysine cyclodeaminase activity.

Using a radiographic TLC-based assay, we observed the time-dependent conversion of L-lysine to L-pipecolic acid in the presence of RapL and NAD^+. In addition, we confirmed the correct stereochemistry of the product by chiral radio-HPLC. RapL exhibited Michaelis−Menten kinetic behavior with respect to L-lysine, yielding a K_m of 46 ± 4 μM, 5- to 100-fold tighter than that observed for OCDs from *C. sporogenes*[23] and *A. tumefaciens*.[26,27] Cyclization of L-ornithine by RapL was also observed, albeit at a significantly reduced rate when compared to the natural substrate. Although saturation kinetics were not observed for L-ornithine, the catalytic efficiency (approximated by k_{cat}/K_m) was reduced 100-fold relative to L-lysine. We did not observe any product formation when D-lysine was added in place of its enantiomer. These data indicate a clear preference for the expected L-lysine substrate, implying that RapL has evolved a high degree of selectivity for alkyl chain length and α-carbon stereochemistry.

The enzymatic logic to convert lysine into the nonproteinogenic monomer pipecolic acid is akin to that used to convert nonproteinogenic ornithine into proline: a cryptic redox process that does not result in net change in the oxidation state between substrate and products (Figure 2C). This strategy is part of a reaction class, the so-called "complex NAD^+-dependent transformations", in which the enzyme binds oxidized nicotinamide so tightly that it typically does not dissociate at the end of each catalytic cycle and, hence, functions as a prosthetic group. To prevent dissociation of reduced cofactor and, as a result, premature termination of the catalytic cycle, one presumes that NADH should bind to the enzyme even more tightly than NAD^+. In parallel, upon oxidation of lysine, the nascent imino acid must be held at the active site long enough to undergo an uninterrupted series of transformations, including intramolecular attack by the ϵ-amine and loss of ammonia from the ensuing tetrahedral adduct to arrive at the cyclic Δ^1-piperideine-2-carboxylate intermediate. Finally, this cyclic imine must be reduced by the nascent NADH in the active site, regenerating the starting oxidation state of the bound nicotinamide (NAD^+) and releasing the product.

For some enzymes that utilize NAD^+ catalytically, including mammalian *S*-adenosylhomocysteine hydrolase,[44] UDP-galactose 4-epimerase,[45] ADP-*β*-L-*glycero*-D-*manno*-heptose 6-epimerase,[46] and TDP-glucose 4,6-dehydratase,[47] no addition of cofactor is necessary for full enzymatic activity, a presumed consequence of tight binding of the prosthetic group in the enzyme active site. However, for other enzymes of this class, including CDP-glucose 4,6-dehydratase,[48] parasitic forms of *S*-adenosylhomocysteine hydrolase,[49,50] dehydroquinate synthase,[51] and the OCDs,[22,26,27] full activity is dependent upon added NAD^+. RapL falls into this latter group, as removal of exogenous NAD^+ from the assay resulted in an 8-fold loss in initial reaction velocity (Figure 5A). The apparent K_m of NAD^+ in the RapL reaction is 2.3 ± 0.4 μM, within a 5-fold range of similar values reported for OCDs.[22,26,27] To further examine the identity of the cofactors bound to RapL, we determined the NAD^+/NADH content of the enzyme using spectroscopic and HPLC-based methods. The absorption spectrum of RapL revealed a peak near 340 nm, consistent with the presence of bound NADH. Quantitation of cofactor content after denaturation and chromatographic analysis indicated that RapL is present in three forms: apo, NAD^+-bound, and NADH-bound.

Given its catalytic mechanism, RapL can falter in at least two ways during a reaction cycle. If the enzyme mistakenly loses nicotinamide cofactor, either starting NAD^+ or intermediate NADH, it will be stranded in a redox incompetent state. Second, if any of the oxidized lysine intermediates diffuse out

(41) Bierer, B. E.; Mattila, P. S.; Standaert, R. F.; Herzenberg, L. A.; Burakoff, S. J.; Crabtree, G.; Schreiber, S. L. *Proc. Natl. Acad. Sci. U.S.A.* **1990**, *87*, 9231−9235.
(42) Motamedi, H.; Shafiee, A. *Eur. J. Biochem.* **1998**, *256*, 528−534.
(43) Wu, K.; Chung, L.; Revill, W. P.; Katz, L.; Reeves, C. D. *Gene* **2000**, *251*, 81−90.
(44) Palmer, J. L.; Abeles, R. H. *J. Biol. Chem.* **1979**, *254*, 1217−1226.
(45) Wilson, D. B.; Hogness, D. S. *J. Biol. Chem.* **1964**, *239*, 2469−2481.
(46) Read, J. A.; Ahmed, R. A.; Morrison, J. P.; Coleman, W. G., Jr.; Tanner, M. E. *J. Am. Chem. Soc.* **2004**, *126*, 8878−8879.
(47) Zarkowsky, H.; Glaser, L. *J. Biol. Chem.* **1969**, *244*, 4750−4756.
(48) He, X.; Thorson, J. S.; Liu, H.-w. *Biochemistry* **1996**, *35*, 4721−4731.
(49) Parker, N. B.; Yang, X.; Hanke, J.; Mason, K. A.; Schowen, R. L.; Borchardt, R. T.; Yin, D. H. *Exp. Parasitol.* **2003**, *105*, 149−158.
(50) Yang, X.; Borchardt, R. T. *Arch. Biochem. Biophys.* **2000**, *383*, 272−280.
(51) Srinivasan, P. R.; Rothschild, J.; Sprinson, D. B. *J. Biol. Chem.* **1963**, *238*, 3176−3182.

of the active site before re-reduction, then the enzyme will be left in the NADH-bound state, incompetent for subsequent catalytic cycles. For RapL overproduced from *E. coli*, both deactivating pathways may be operant. As isolated, RapL has only 0.5 equiv of nicotinamide bound, only one-third of which is bound to NAD^+. While exogenous addition of NAD^+ can stimulate turnover, it is not yet clear what fraction of bound NADH may be displaced and, hence, what enzyme fraction may be converted back to competency by added NAD^+. Presumably, the exogenous addition of Δ^1-piperideine-2-carboxylate would regenerate all the NADH-occupied RapL sites.

These two problems are not unique to RapL but show up to different extents in other members of this class of enzymes containing tightly bound, nondissociable NAD^+ with redox reactions occult in the overall stoichiometry. For example, a similar mixture of apo and holo forms has been reported for CDP-glucose 4,6-hydratase.[48] In addition, Frey and co-workers demonstrated that full activity of UDP-galactose 4-epimerase could only be achieved after mild denaturation of the protein and replacement of any bound NADH with NAD^+.[52] Further dissection of these issues for RapL would be greatly aided by the preparation of enzyme entirely in its apo form.

Using isotopically labeled substrates, postreaction Fmoc derivatization, reversed-phase HPLC purification, and LTQ-FT mass spectrometry, we have examined two aspects of this mechanism: (a) loss of the amine at the α-position and (b) retention of the hydrogen atom on the α-carbon. When RapL was incubated in the presence of lysine labeled with ^{15}N at the α-position, no mass shift was observed in the purified pipecolic acid product. However, when the label was present at the ϵ-position, the mass of the corresponding product was greater than the unlabeled standard by 1 Da. These data clearly indicate that the ϵ-NH_2 is retained during the course of the cyclization, while the α-NH_2 is likely lost as ammonia, consistent with the observations of *P. putida* OCD by Muth and Costilow.[24] To determine if hydrogen exchange with solvent at the α-carbon occurs, we incubated RapL with a form of lysine in which each carbon-bound hydrogen has been replaced with deuterium. If hydrogen exchange at the α-position (or at any other carbon) of lysine does occur, one would expect the mass of the pipecolic acid product to be lighter by at least 1 Da. However, for this experiment, the observed mass of the pipecolic acid product is consistent with retention of all nine deuterium atoms. This observation strongly suggests that the deuterium abstracted from the α-position of the substrate and transferred to NAD^+ is the same as that returned to the cyclic imino acid intermediate from the transiently formed 4-[^{2}H]NADH.

There has been much interest in the generation of biologically active variants of rapamycin and FK506/FK520. One general strategy toward the generation of such compounds has focused on the alteration of the biosynthetic pathway by genetic[53] or chemical[54] methods such that a requisite intermediate is no longer produced. The bacterial strain is then supplemented with analogues of the missing intermediate that can still be utilized by the biosynthetic enzymes. This technique, precursor-directed biosynthesis, has been applied to RapL both by genetic disruption[19] and by the treatment of producer strain with presumed cyclodeaminase inhibitors: (±)-nipecotic acid[35,36] and (±)-thiazolidine-2-carboxylic acid (T2CA).[34] To determine the in vitro effectiveness of these compounds as RapL inhibitors, we measured dose−response curves for the two stereoisomers of nipecotic acid and T2CA over a broad range of inhibitor concentrations. T2CA exhibited the lowest IC_{50} at 96 μM. As one would expect based on the stereospecificity of the RapL reaction, the two stereoisomers of nipecotic acid displayed different activities, with an IC_{50} for (*S*)-(+)-nipecotic acid approximately 7-fold lower than that of its enantiomer (680 μM versus 4.8 mM). While all three compounds did impair cyclodeaminase activity to varying degrees, their relatively modest IC_{50} values leave open the possibility that more effective RapL inhibitors have yet to be characterized.

Acknowledgment. This work was supported by grants from the National Institutes of Health (GM020011 (to C.T.W.), GM067725 (to N.L.K.), F32GM069169 (to G.J.G.), and T32GM07283 (to M.T.B.)). We thank Christopher D. Reeves at Kosan Biosciences for providing the *rapL*-containing cosmid, and Annaleise Howard-Jones and Ellen Yeh for helpful discussions and critical reading of the manuscript.

JA0587603

(52) Liu, Y.; Vanhooke, J. L.; Frey, P. A. *Biochemistry* **1996**, *35*, 7615−7620.
(53) Weist, S.; Sussmuth, R. D. *Appl. Microbiol. Biotechnol.* **2005**, *68*, 141−150.
(54) Thiericke, R.; Rohr, J. *Nat. Prod. Rep.* **1993**, *10*, 265−289.